

Synthesis and Structural Characterization of Molecular Dy(III) and Er(III) Tetra-Carbonates

George S. Goff,^{*,†} Michael R. Cisneros,[†] Chandra Kluk,[†] Kevin Williamson,[†] Brian Scott,[‡] Sean Reilly,[†] and Wolfgang Runde^{*,§}

[†]Chemistry Division, [‡]Materials Physics and Applications Division, and [§]Science Program Office, Los Alamos National Laboratory, Los Alamos, New Mexico 87545

Received March 9, 2010

Single crystal structures of lanthanide carbonate and hydroxy-carbonate compounds have been previously reported in the literature, with the majority of these compounds being extended one- to three-dimensional compounds. Very few lanthanide compounds have been isolated that contain molecular moieties, and none have been reported for either erbium or dysprosium. Single crystals of the tetra-carbonate complexes, $[\text{C}(\text{NH}_2)_3]_5[\text{Er}(\text{CO}_3)_4] \cdot 11\text{H}_2\text{O}$ (I) and $[\text{C}(\text{NH}_2)_3]_4[\text{Dy}(\text{CO}_3)_4(\text{H}_2\text{O})](\text{H}_3\text{O}) \cdot 13\text{H}_2\text{O}$ (II), were isolated from concentrated guanidinium carbonate solutions and characterized by single crystal X-ray diffraction studies. Compounds I and II are the first reported molecular carbonate structures for Er and Dy to be characterized via single crystal X-ray diffraction studies. Crystallographic data for I: monoclinic, space group $P2_1/n$, $a = 8.8160(6)$ Å, $b = 21.0121(14)$ Å, $c = 19.6496(14)$ Å, $Z = 4$. Data for II: tetragonal, space group $P4/n$, $a = b = 15.3199(11)$ Å, $c = 7.5129(11)$ Å, $Z = 2$.

Introduction

The light lanthanides (Ln) are important fission products in used nuclear fuel with potential impacts for both the recycling of used fuel in advanced nuclear fuel cycles, as well as for the stability of waste forms to be disposed in nuclear waste repositories. Due to their similar chemistries in solution and the solid state, the trivalent lanthanides are often used as surrogates for predicting the chemistry and environmental fate of the highly radioactive and long-lived isotopes of the trivalent actinides. The geochemistry and fate of both actinides and lanthanides in the environment is closely linked to carbonate, which is abundant and known to be a strongly coordinating ligand for both the 4f and 5f elements. Over the past three decades, significant research has been performed on the solubility and solution speciation of the lanthanides (and actinides) in the presence of carbonate; however, little is known about the coordination chemistry of lanthanides in environmentally relevant compounds. The crystal chemistry of the known Ln-carbonate compounds has been thoroughly reviewed by Wickleder,¹ including binary lanthanide carbonate compounds as well as hydroxy-carbonate and fluoro-carbonate compounds. Most of the reported solid state carbonates were characterized by powder X-ray diffraction

studies, spectroscopic methods, and thermal/gravimetric analysis.^{1–9} The overwhelming majority of lanthanide carbonates reported in the literature consist of extended multi-dimensional arrays. In fact, the only two molecular structures for Ln(III)-carbonate compounds reported in the literature are $[\text{C}(\text{NH}_2)_3]_5[\text{Nd}(\text{CO}_3)_4(\text{H}_2\text{O})] \cdot 2\text{H}_2\text{O}$ ¹⁰ and $[\text{Co}(\text{NH}_3)_6]_6[\text{Na}_2(\text{H}_2\text{O})_{10}][\text{Ho}(\text{CO}_3)_4] \cdot 4\text{H}_2\text{O}$,¹¹ both containing the Ln- $(\text{CO}_3)_4^{5-}$ anion as a molecular building block.

The solid carbonates of the lanthanides exhibit a range of stoichiometries, from $\text{Ln}_2(\text{CO}_3)_3 \cdot n\text{H}_2\text{O}$ in the normal carbonates¹² to $\text{MLn}(\text{CO}_3)_2 \cdot n\text{H}_2\text{O}$,⁴ $\text{MLn}(\text{CO}_3)_3(\text{H}_2\text{O}) \cdot n\text{H}_2\text{O}$,¹³ $\text{M}_3\text{Ln}(\text{CO}_3)_3$,^{9,14,15} $\text{M}_5\text{Ln}(\text{CO}_3)_4 \cdot n\text{H}_2\text{O}$,¹¹ and

- (4) Mochizuki, A.; Nagashima, K.; Wakita, H. *Bull. Chem. Soc. Jpn.* **1974**, *47*, 755.
- (5) Nagashima, K.; Wakita, H.; Mochizuki, A. *Bull. Chem. Soc. Jpn.* **1973**, *46*, 152.
- (6) Dexpert, H.; Caro, P. *Mater. Res. Bull.* **1974**, *9*, 1577.
- (7) Philippini, V.; Vercouter, T.; Chausse, A.; Vitorge, P. *J. Solid State Chem.* **2008**, *181*, 2143.
- (8) Gu, F.; Wang, Z.; Han, D.; Guo, G.; Guo, H. *Cryst. Growth Des.* **2007**, *7*, 1452.
- (9) Ben Ali, A.; Maisonneuve, V.; Houlbert, S.; Silly, G.; Buzare, J. Y.; Leblanc, M. *Solid State Sci.* **2004**, *6*, 1237.
- (10) Runde, W.; Neu, M. P.; Van Pelt, C.; Scott, B. L. *Inorg. Chem.* **2000**, *39*, 1050.
- (11) Bond, D. L.; Clark, D. L.; Donohoe, R. J.; Gordon, J. C.; Gordon, P. L.; Keogh, D. W.; Scott, B. L.; Tait, C. D.; Watkin, J. G. *Eur. J. Inorg. Chem.* **2001**, 2921.
- (12) Shinn, D. B.; Eick, H. A. *Inorg. Chem.* **1968**, *7*, 1340.
- (13) Clark, D. L.; Donohoe, R. J.; Gordon, J. C.; Gordon, P. L.; Keogh, D. W.; Scott, B. L.; Tait, C. D.; Watkin, J. G. *Dalton* **2000**, 1975.
- (14) Mercier, N.; Leblanc, M.; Antic-Fidancev, E.; Lemaitre-Blaise, M. *J. Solid State Chem.* **1997**, *132*, 33.
- (15) Saito, A.; Ueno, K. *J. Inorg. Nucl. Chem.* **1979**, *41*, 513.

*To whom correspondence should be addressed. E-mail: georgeg@lanl.gov or runde@lanl.gov.

(1) Wickleder, M. S. *Chem. Rev. (Washington, DC, U. S.)* **2002**, *102*, 2011.
(2) Christensen, A. N. *Acta Chem. Scand. (1947–1973)* **1973**, *27*, 2973.
(3) Christensen, A. N.; Hornreich, R. M.; Sharon, B. *Solid State Commun.* **1973**, *13*, 963.

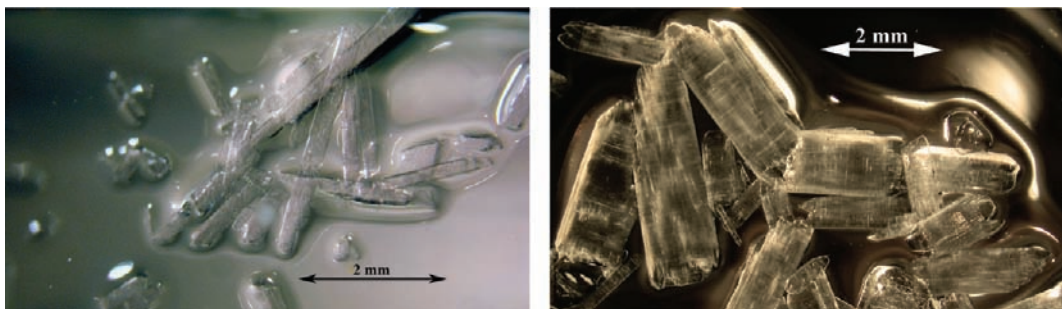


Figure 1. Pictures showing the rectangular plates of single crystal $[C(NH_2)_3]_3[Er(CO_3)_4] \cdot 11H_2O$ (I) (left) and $[C(NH_2)_3]_4[Dy(CO_3)_4(H_2O)](H_3O) \cdot 13H_2O$ (II) (right).

$M_5Ln(CO_3)_4(H_2O) \cdot nH_2O$ ¹⁰ in the double salts. Higher stoichiometries have been observed only for cerium, which forms the pentacarbonate compound $M_6Ce(CO_3)_5 \cdot nH_2O$.^{16–18} Solubility and spectroscopic data have been interpreted predominantly with the complexes $Ln(CO_3)_n^{3-2n}$ where $n = 0–3$. The limiting solution species for trivalent f elements has been widely debated in the literature, and two stoichiometries, $M(CO_3)_3^{3-19-21}$ and $M(CO_3)_4^{5-}$, have been proposed depending on the solution conditions ($[CO_3^{2-}]$, pH, ionic strength, etc.).^{20,22–24} Although such complexes require increased concentrations of carbonate and are less relevant for general environmental conditions (with millimolar or less in carbonate), they are important for used fuel reprocessing under alkaline conditions and the separation and purification of americium and curium from their chemically analogous lanthanides.

Our research group has been focused on understanding and exploiting the differences in the solubility and speciation behavior of transition metal, lanthanide, and actinides in alkaline carbonate media to develop a new alkaline-based separation process for used nuclear fuel reprocessing.^{25–27} Our explorations into the coordination chemistry of f element compounds in alkaline solutions (CO_3^{2-} and OH^-) with known radiolysis products (H_2O_2 , oxalate, etc.) have provided

a rich canvas for unique molecular structures of actinide and lanthanide solution complexes.^{28–31} These compounds provide insight into the fundamental behavior and electronic structure of f element complexes and may hint toward structural motifs of compounds not yet structurally characterized. To this aim, we have been studying the behavior of the Ln(III) elements in concentrated carbonate solutions, and we report herein the first molecular structure for Er and Dy carbonates.

Experimental Methods

Guanidinium carbonate (99+% purity) solutions were allowed to equilibrate over several days at room temperature to ensure saturation. Lanthanide stock solutions were prepared gravimetrically by dissolving $Dy(NO_3)_3 \cdot 6H_2O$ (99.99% purity) and $Er(NO_3)_3 \cdot 6H_2O$ (99.99% purity) in water. Chemicals were purchased from Fisher Scientific, Inc., and all solutions were prepared from distilled deionized water with a specific resistance $\geq 18.0 M\Omega \cdot cm$.

Single crystals of **I** and **II** were prepared by adding varying amounts of the Ln(III) nitrate stock to saturated guanidinium carbonate solutions. Aliquots of the Er and Dy stock solutions were added in excess of 40 mM under vigorous stirring, and solutions were then filtered through a $0.45 \mu m$ polyamide syringe filter and transferred to a 4 mL borosilicate scintillation vial. Solutions were evaporated at $3^\circ C$ to allow for slow crystallization of **I** and **II**, which are shown in Figure 1. The crystal structures were obtained by using single crystal X-ray diffraction studies, while additional characterization was performed using conventional Raman and UV–vis–NIR spectroscopy. Solid samples of **I** and **II** were ground, and spectra were collected with a Cary 5 UV–vis–NIR spectrophotometer with a diffuse reflectance attachment. Raman spectra were measured with a Nicolet Magna-IR 560 ESD equipped with a Raman accessory.

Crystallographic Studies. Single crystals of **I** and **II** were removed from the remaining guanidinium carbonate solution and characterized by single crystal X-ray diffraction studies. Crystals were mounted in turn using a nylon cryoloop and Paratone-N oil. The data were collected on a Bruker D8 diffractometer, with an APEX II charge-coupled-device (CCD) detector, and a Bruker Kryoflex low temperature device. The instrument was equipped with a graphite monochromatized $Mo K\alpha$ X-ray source ($\lambda = 0.71073 \text{ \AA}$) and a 0.5 mm monocapillary. A hemisphere of data was collected using ω scans, with 10-s frame exposures and 0.5° frame widths. Data collection and initial indexing and cell refinement were handled using APEX II software.³² Frame integration, including Lorentz-polarization corrections, and final cell parameter calculations were carried out using SAINT+ software.³³ The data were corrected for

(16) Dervin, J.; Faucherre, J.; Herpin, P.; Voliotis, S. *Bull. Soc. Chim. Fr.* **1973**, 2634.

(17) Voliotis, S.; Rimsky, A.; Faucherre, J. *Acta Crystallogr., Sect. B* **1975**, *B31*, 2607.

(18) Voliotis, S.; Rimsky, A. *Acta Crystallogr., Sect. B* **1975**, *B31*, 2620.

(19) Kim, J. I.; Klenze, R.; Wimmer, H.; Runde, W.; Hauser, W. *J. Alloys Compd.* **1994**, *213/214*, 333.

(20) Philippini, V.; Vercouter, T.; Aupiais, J.; Topin, S.; Ambard, C.; Chausse, A.; Vitorge, P. *Electrophoresis* **2008**, *29*, 2041.

(21) Vercouter, T.; Vitorge, P.; Trigoulet, N.; Giffaut, E.; Moulin, C. *New J. Chem.* **2005**, *29*, 544.

(22) Rao, R. R.; Chatt, A. *Radiochim. Acta* **1991**, *54*, 181.

(23) Sinha, S. P. *Fresenius. Z. Anal. Chem.* **1982**, *313*, 238.

(24) Dumonceau, J.; Bigot, S.; Treuil, M.; Faucherre, J.; Fromage, F. *Rev. Chim. Miner.* **1979**, *16*, 583.

(25) Peper, S. M.; Brodnax, L. F.; Field, S. E.; Zehnder, R. A.; Valdez, S. N.; Runde, W. H. *Ind. Eng. Chem. Res.* **2004**, *43*, 8188.

(26) Goff, G. S.; Brodnax, L. F.; Cisneros, M. R.; Taw, F. L.; Williamson, K. S.; Runde, W. H. Abstracts of Papers, 234th ACS National Meeting, Boston, MA, United States, August 19–23, 2007, INOR.

(27) Runde, W.; Villarreal, R.; Jarvinen, G. Abstracts of Papers, 233rd ACS National Meeting, Chicago, IL, United States, March 25–29, 2007, NUCL.

(28) Goff, G. S.; Brodnax, L. F.; Cisneros, M. R.; Peper, S. M.; Field, S. E.; Scott, B. L.; Runde, W. H. *Inorg. Chem.* **2008**, *47*, 1984.

(29) Runde, W.; Brodnax Lia, F.; Goff George, S.; Peper Shane, M.; Taw Felicia, L.; Scott Brian, L. *Chem. Commun. (Cambridge, U. K.)* **2007**, 1728.

(30) Zehnder, R. A.; Batista, E. R.; Scott, B. L.; Peper, S. M.; Goff, G. S.; Runde, W. H. *Radiochim. Acta* **2008**, *96*, 575.

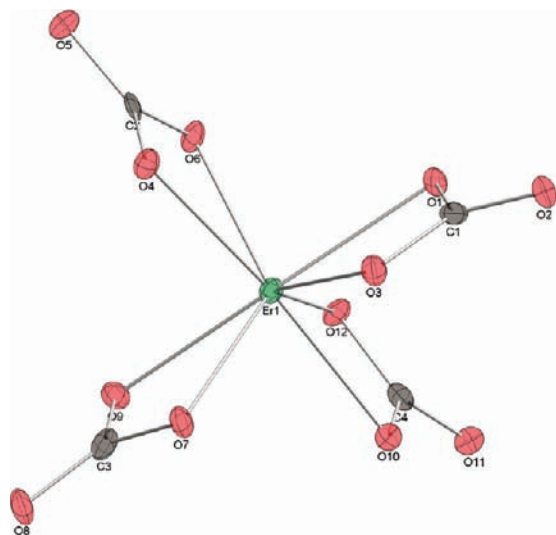
(31) Zehnder, R. A.; Peper, S. M.; Scott, B. L.; Runde, W. H. *Acta Crystallogr., Sect. C* **2005**, *C61*, i3.

(32) APEX II; Bruker AXS, Inc.: Madison, WI, 2004.

(33) SAINT+; Bruker AXS, Inc.: Madison, WI, 2003.

Table 1. Crystallographic Data for $[\text{C}(\text{NH}_2)_3]_5[\text{Er}(\text{CO}_3)_4] \cdot 11\text{H}_2\text{O}$ (I) and $[\text{C}(\text{NH}_2)_3]_4[\text{Dy}(\text{CO}_3)_4(\text{H}_2\text{O})](\text{H}_3\text{O}^+) \cdot 13\text{H}_2\text{O}$ (II)

	$[\text{C}(\text{NH}_2)_3]_5[\text{Er}(\text{CO}_3)_4] \cdot 11\text{H}_2\text{O}$ (I)	$[\text{C}(\text{NH}_2)_3]_4[\text{Dy}(\text{CO}_3)_4(\text{H}_2\text{O})](\text{H}_3\text{O}^+) \cdot 13\text{H}_2\text{O}$ (II)
fw (g/mol)	905.92	998.12
<i>a</i> (Å)	8.8160(6)	15.3199(11)
<i>b</i> (Å)	21.0121(14)	15.3199(11)
<i>c</i> (Å)	19.6496(14)	7.5129(11)
α (deg)	90.00	90.00
β (deg)	94.3980(10)	90.00
γ (deg)	90.00	90.00
volume (Å ³)	3629.2(4)	1763.3(3)
Z	4	2
R-factor %	5.74	8.09
space group	<i>P</i> 21/ <i>n</i>	<i>P</i> 4/ <i>n</i>
system	monoclinic	tetragonal

**Figure 2.** Thermal ellipsoid (50% probability) plot of the erbium coordination and atomic numbering scheme in $[\text{C}(\text{NH}_2)_3]_5[\text{Er}(\text{CO}_3)_4] \cdot 11\text{H}_2\text{O}$ (I).

absorption using redundant reflections and the SADABS program.³⁴ Decay of reflection intensity was not observed as monitored via analysis of redundant frames. The structure was solved using direct methods and difference Fourier techniques. Hydrogen atom positions were not considered in the final model due to the difficulty of locating and refining water hydrogen atom positions in a heavy atom structure. Compound II had four disordered water molecules per unit cell and were treated using the program PLATON/SQUEEZE.³⁵ The residual electron density before squeezing was not consistent with additional guanidinium cations. The final refinement included anisotropic temperature factors on all non-hydrogen atoms. Structure solution, refinement, and creation of publication materials were performed using SHELXTL.³⁶ Table 1 shows the important crystallographic parameters for both I and II. Complete crystallographic details can be found in the Supporting Information.

Results and Discussion

Structure and Characterization of $[\text{C}(\text{NH}_2)_3]_5[\text{Er}(\text{CO}_3)_4] \cdot 11\text{H}_2\text{O}$. The molecular structure of I is comprised of discrete $\text{Er}(\text{CO}_3)_4^{5-}$ anionic units linked through interactions with lattice waters and guanidinium

Table 2. Selected Bond Distances (Å) and Angles (deg) for $[\text{C}(\text{NH}_2)_3]_5[\text{Er}(\text{CO}_3)_4] \cdot 11\text{H}_2\text{O}$ (I)

Er1—O1	2.349(4)
Er1—O10	2.324(4)
Er1—O12	2.355(4)
Er1—O3	2.330(4)
Er1—O4	2.342(5)
Er1—O6	2.302(4)
Er1—O7	2.341(4)
Er1—O9	2.333(4)
Er1—C1	2.748(7)
Er1—C2	2.726(7)
Er1—C3	2.754(8)
Er1—C4	2.753(7)
O1—Er1—O3	56.32(16)
O4—Er1—O6	56.39(16)
O7—Er1—O9	56.15(15)
O10—Er1—O12	56.27(15)
C1—Er1—C3	138.8(2)
C2—Er1—C4	133.0(2)
C1—Er1—C2	103.97(18)
C1—Er1—C4	92.7(2)
C2—Er1—C3	94.6(2)
C3—Er1—C4	104.08(19)

cations $[\text{C}(\text{NH}_2)_3]^+$. Figure 2 shows the atom numbering and thermal ellipsoid plot for a single polyhedron of I, while Table 2 lists selected bond lengths and angles. The monoclinic unit cell contains one $\text{Er}(\text{CO}_3)_4^{5-}$ anion, five guanidinium cations, and 11 lattice waters, with the eight-coordinate Er atom bound to oxygen atoms from four bidentate carbonate ligands. Although the $\text{Er}(\text{CO}_3)_4^{5-}$ anion does not occupy a position of crystallographic symmetry, it does have approximate C_{2v} point group symmetry. The average Er—O bond length is 2.335(4) Å and varies between 2.324(4) and 2.355(4) Å. This is somewhat shorter than the reported Er—O_{carbonate} bond lengths found in the extended three-dimensional structures $\text{Er}(\text{CO}_3)\text{OH}$ (2.412–2.495 Å)³⁷ and $\text{Er}_2(\text{CO}_3)_2(\text{C}_2\text{O}_4) \cdot 2\text{H}_2\text{O}$ (2.404–2.448 Å).³⁸ The much longer Er—O bond length in the hydroxycarbonate compound can be explained by the reported monodentate carbonate ligands, while the mixed oxalate—mononate $\text{Er}(\text{III})$ compound contains solely bidentately coordinated carbonate ligands like I. In both structures, the carbonate ligands form bridges between Er atoms in an extended network, which likely increases the Er—O_{carbonate} bond length compared to that in the molecular structure of I.

The bite angles of the bound carbonates in I show little variation, with an average O—Er—O angle of 56.28(16)°. This compares well to the O—Er—O angles of 53.07° and 53.83° found in $\text{Er}_2(\text{CO}_3)_2(\text{C}_2\text{O}_4) \cdot 2\text{H}_2\text{O}$.³⁸ The average Er—C distance is 2.745(7) Å, and *trans*-carbonate ligands are distorted significantly out of plane such that the C—Er—C angles are 138.8(2) and 133.0(2)° for C1—Er—C3 and C2—Er—C4, respectively. The lack of planarity of the *trans*-carbonates was also observed to a greater degree in the holmium compound $[\text{Co}(\text{NH}_3)_6][\text{Na}_2(\text{H}_2\text{O})_{10}][\text{Ho}(\text{CO}_3)_4] \cdot 4\text{H}_2\text{O}$, which has a *trans*-C—Ho—C angle of 132.26(10)°. The wide range of the C—Er—C angles for the *cis*-carbonates in I, 92.7(2)–104.08(19)°, indicates an extreme deviation from the ideal tetragonal geometry and results in a distorted bicapped trigonal prism.³⁹

(34) Sheldrick, G. *SADABS*; University of Gottingen: Gottingen, Germany, 2001.

(35) Spek, A. L. *Acta Crystallogr.* **1990**, *A46*, C34.

(36) *SHELXTL*; Bruker AXS, Inc.: Madison, WI, 1997.

(37) Tahara, T.; Nakai, I.; Miyawaki, R.; Matsubara, S. *Z. Kristallogr.* **2007**, *222*, 326.

(38) Mueller-Buschbaum, K. *Z. Anorg. Allg. Chem.* **2002**, *628*, 1761.

(39) Haigh, C. W. *Polyhedron* **1995**, *14*, 2871.

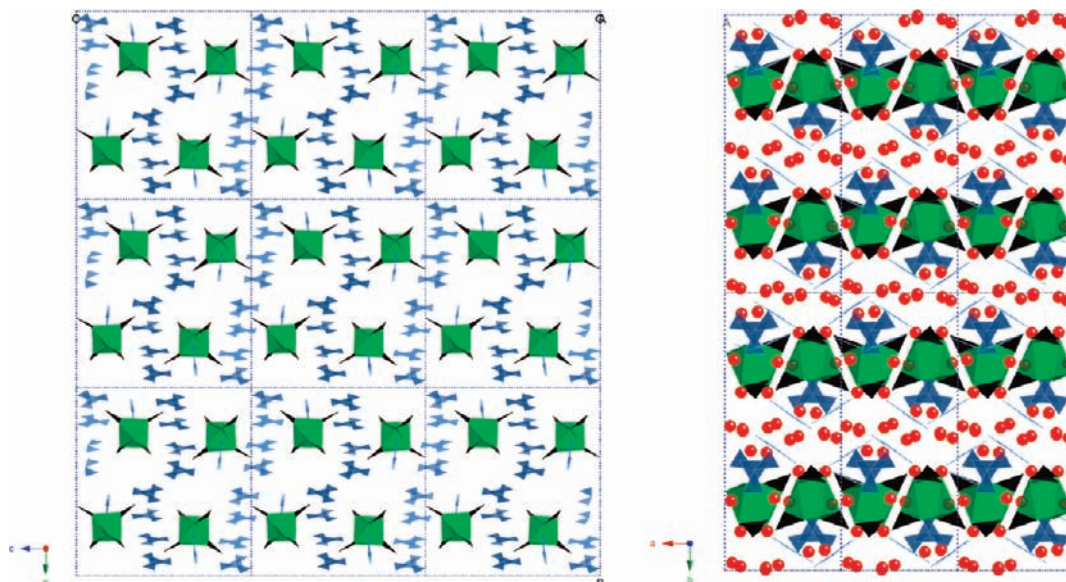


Figure 3. Illustration of the packing in the molecular structure of [C(NH₂)₃]₅[Er(CO₃)₄]·11H₂O (**I**) along the *a* axis (left) and *c* axis (right). Water molecules are denoted by red spheres, green polyhedra indicate [ErO₈] groups, black triangles indicate [CO₃] groups, and light blue groups represent guanidinium groups [C(NH₂)₃]. For clarity, water molecules have been omitted from the view along the *a* axis (left).

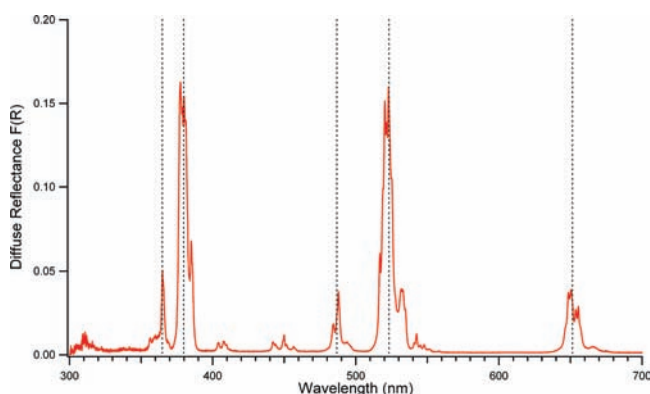


Figure 4. Spectroscopic features of the UV–vis–NIR diffuse reflectance spectrum (solid line) of [C(NH₂)₃]₅[Er(CO₃)₄]·11H₂O (**I**) indicate small shifts in the primary absorbance peaks relative to the five most intense transitions in the Er³⁺ aquo ion absorbance spectrum (dashed line).⁴⁰

The anionic units of **I** are linked together by an extended network of hydrogen bonding between the guanidinium cations, lattice waters, and carbonate ligands, as shown in Figure 3. The [ErO₈] polyhedra and guanidinium cations are stacked in columns along the *a* axis. These stacks of [ErO₈] polyhedra are separated by ribbons of guanidinium cations stacked along the *b* axis in the *bc* plane. Five of the lattice waters (O6W and O8W–O11W) form a two-dimensional network in the *ac* plane, and each water layer separates the layers of [ErO₈] polyhedra in the *ab* plane. The four water molecules closest to the Er(CO₃)₄⁵⁻ anion, O1W, O2W, O3W, and O4W, form bridging hydrogen bonds between adjacent Er polyhedra along the *a* axis. While O8W is too far away to interact with the coordinated carbonates (closest distance to O_{carb} is 4.009 Å), it does interact with two other lattice waters and two guanidinium cations.

Additional characterization of **I** was performed by using conventional UV–vis–NIR diffuse reflectance

spectroscopy. The electronic absorbance spectrum for Er³⁺ is characterized by a number of Laporte-forbidden *f*–*f* transitions in the visible region from 400 to 800 nm.⁴⁰ Figure 4 shows a comparison of the solid state diffuse reflectance spectrum for **I** and the significant *f*–*f* transitions in the Er³⁺ aquo ion absorbance spectrum. Several strong absorbance peaks for [C(NH₂)₃]₅[Er(CO₃)₄]·11H₂O can be found at 365.0, 377.4, 380.0, 487.9, 520.3, 521.6, 522.9, 648.6, and 650.3 nm. This shows good agreement with the strongest peaks in the aquo ion (in order of decreasing intensity) at 379, 523, 364, 487, and 652 nm,⁴⁰ with only slight shifts in the peak maxima resulting from Er complexation with the carbonate ligands.

Structure and Characterization of [C(NH₂)₃]₄[Dy(CO₃)₄(H₂O)](H₃O)·13H₂O. The structure of **II** is similar to that of **I**, with discrete Dy(CO₃)₄(H₂O)⁵⁻ anionic units linked through interactions of the carbonate ligands with lattice water molecules and guanidinium cations. In contrast to the eight-coordinate Er atom in **I**, Dy is bound to nine oxygen atoms in **II**, with eight O's from four bidentately coordinated carbonate ligands and one O from a bound water molecule. This nine-coordinate geometry is consistent with the previously reported neodymium structure, [C(NH₂)₃]₅[Nd(CO₃)₄(H₂O)]·2H₂O, which includes the isostructural anionic unit [Nd(CO₃)₄(H₂O)]⁵⁻.¹⁰ Figure 5 shows the thermal ellipsoid plot for a single polyhedron of **I**, while Table 3 lists selected bond lengths and angles. The unit cell is tetragonal and contains the Dy(CO₃)₄(H₂O)⁵⁻ anion, four guanidinium cations, and 13 lattice waters and one hydronium ion. The anionic unit in **II** occupies a 4-fold rotation axis, which contains the Dy atom and the bound water oxygen atom (O4). The approximate point group symmetry of the anionic unit is C₄. The [DyO₉] polyhedron is a mono-capped antiprism, with the eight oxygen atoms from the bound carbonate ligands forming the corners of the square

(40) Carnall, W. T. *Handb. Phys. Chem. Rare Earths* **1979**, 3, 171.

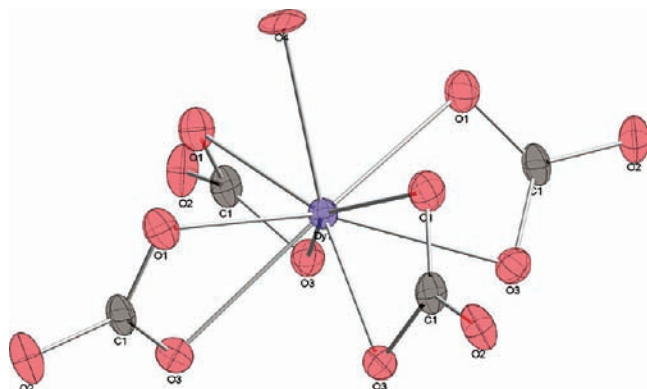


Figure 5. Thermal ellipsoid (50% probability) plot of the dysprosium coordination and atomic numbering scheme in $[\text{C}(\text{NH}_2)_3]_4[\text{Dy}(\text{CO}_3)_4(\text{H}_2\text{O})](\text{H}_3\text{O}) \cdot 13\text{H}_2\text{O}$ (**II**).

Table 3. Selected Bond Distances (Å) and Angles (deg) for $[\text{C}(\text{NH}_2)_3]_4[\text{Dy}(\text{CO}_3)_4(\text{H}_2\text{O})](\text{H}_3\text{O}) \cdot 13\text{H}_2\text{O}$ (**II**)

Dy1—O1	2.378(7)
Dy1—O3	2.422(6)
Dy1—O4	2.444(12)
Dy1—C1	2.805(9)
O1—Dy1—O1	146.7(4)
O1—Dy1—O1	85.30(10)
O1—Dy1—O3	53.3(2)
O1—Dy1—O3	152.9(2)
O1—Dy1—O3	120.0(2)
O1—Dy1—O3	78.1(2)
C1—Dy1—C1 (<i>trans</i>)	166.2(5)

antiprism and the water molecule capping the top. The $\text{Dy}-\text{O}_{\text{carbonate}}$ bond length is either 2.378(7) or 2.422(6) Å, which is longer than the average $\text{Er}-\text{O}_{\text{carbonate}}$ bond length of 2.745(7) Å in **I**. Nevertheless, this distance is similar to the $\text{Ln}-\text{O}_{\text{carbonate}}$ distance for bidentately coordinated carbonates found in the light Ln complexes $[\text{C}(\text{NH}_2)_3]_5[\text{Nd}(\text{CO}_3)_4(\text{H}_2\text{O})] \cdot 2\text{H}_2\text{O}$ (2.452(3)–2.544(3) Å),¹⁰ $[\text{Co}(\text{NH}_3)_6][\text{Sm}(\text{CO}_3)_3(\text{H}_2\text{O})] \cdot 4\text{H}_2\text{O}$ (2.745(7)–2.335(4) Å),¹³ and $\text{Na}_3\text{Eu}(\text{CO}_3)_3$ (2.433–2.525 Å).¹⁴ Several Dy compounds have been reported that contain bidentately coordinated carbonate ligands. For instance, the $\text{Dy}-\text{O}_{\text{carbonate}}$ bond lengths in **II** compare very well with those found in $\text{KDy}(\text{CO}_3)_2$ (2.393(5)–2.500(5) Å),⁴¹ and $\text{Dy}_2(\text{O}_2)(\text{CO}_3)$ (2.401(2)–2.557(3) Å).⁴² Multiple polymorphs of the hydroxycarbonate complex $\text{Dy}(\text{OH})(\text{CO}_3)$ have been reported, with the bidentate $\text{Dy}-\text{O}_{\text{carbonate}}$ bond lengths ranging from 2.370(6) to 2.648(4) Å.^{37,42,43} The elongated bond for $\text{Dy}-\text{O}$ in $\text{Dy}(\text{OH})(\text{CO}_3)$ can be explained by the bridging coordination of carbonates between Dy atoms to form a multidimensional network. The shorter $\text{Dy}-\text{O}$ bond length found in **II** is in agreement with other $\text{Ln}-\text{O}$ distances found in molecular Ln carbonate structures (Nd,¹⁰ Ho,¹¹ and **I**) where carbonates are not shared between the Ln atoms.

The bite angle (O1–Dy–O3) of the bound carbonate ligand is 53.2(2)°, which is lower than the bite angles in **I**, as expected due to the increased steric hindrance from the additional bound water molecule. The bite angle in **II** is

nearly identical to the O–Dy–O angle of 53.4° reported in $\text{KDy}(\text{CO}_3)_2$ ⁴¹ and also compares well to the bite angle in the Dy(III) hydroxycarbonate ranging from 48.6 to 53.8°.^{37,42,43} The average Dy–C distance is 2.805(9) Å, and *trans*-carbonate ligands are only distorted slightly out of plane such that the C–Dy–C angle is 166.2(5)°. The $\text{Dy}(\text{CO}_3)_4(\text{H}_2\text{O})^{5-}$ anion is more symmetrical than its Nd analogue, whose *trans*-carbonate ligands are bent more out of plane with C–Nd–C angles of 173 and 155°. As in **I**, the carbonate ligands and the bound water are involved in an extended network of hydrogen bonding interactions between lattice waters and the guanidinium cations, as shown in Figure 6.

Discrete $[\text{DyO}_9]$ polyhedra of the anionic unit are stacked in columns along the *a* axis with the terminal water molecule (Dy–O4) oriented along the *c* axis, and the guanidinium cations are stacked in columns along the *c* axis. Columns of $[\text{DyO}_9]$ units are separated by clusters of guanidinium cations in the *ac* plane, while the guanidinium cations are staggered with the Dy polyhedra along the *a* axis to form a channel with the terminal oxygen (O2) from two *trans*-carbonate ligands lying in the center. Sheets of water molecules separate both the columns of Dy polyhedra and guanidinium clusters along the *b* axis. In the *ab* plane, each $[\text{DyO}_9]$ polyhedron is surrounded by four guanidinium cations, which are situated between two *cis*-carbonate ligands and connect the $[\text{DyO}_9]$ polyhedra by a system of hydrogen bonds to the carbonate ligands.

The most interesting aspect of **II** is the apical Dy–H₂O bond. For charge balance, a neutral bound water molecule requires one hydronium ion in the lattice, while a coordinated hydroxide ligand would require the existence of two hydronium ions to maintain charge neutrality in the unit cell. The Dy–O4 bond length of 2.444(12) Å is the longest of the nine coordinated oxygen atoms. Single crystal structures have been reported for the Dy nonaqua ion with two different counterions, $[\text{Dy}(\text{H}_2\text{O})_9][\text{CF}_3\text{SO}_3]_3$ and $[\text{Dy}(\text{H}_2\text{O})_9][\text{C}_2\text{H}_5\text{SO}_4]_3$.^{44,45} The nine coordinated water molecules in these structures have Dy–O_{water} bond lengths of 2.363(2)–2.520(2) Å and 2.371(1)–2.517(3) Å, respectively, the Dy–OH bond lengths in Dy(III) hydroxide ($\text{Dy}(\text{OH})_3$) range from 2.429(3) to 2.452(3) Å⁴⁶ and fall within the bond length range of the Dy–O_{water} reported for the previous compounds. In contrast, the Dy–OH bond in the mixed hydroxy–carbonate compound $\text{Dy}(\text{OH})\text{CO}_3$ is significantly shorter, ranging from 2.265(3) to 2.415(6) Å.^{37,42,43} A recent review of lanthanide coordination chemistry included an analysis of average bond lengths for compounds containing one coordinated water molecule.⁴⁷ The authors concluded that the average Dy–O_{water} bond length for known compounds was 2.418 Å, which is very close to the Dy–O4 bond length in **II**. In fact, the bond length of 2.444(12) Å in **II** most closely matches the average value for Gd (2.445 Å) reported

(44) Chatterjee, A.; Maslen, E. N.; Watson, K. J. *Acta Crystallogr., Sect. B* **1988**, *B44*, 381.

(45) Gerkin, R. E.; Reppart, W. J. *Acta Crystallogr., Sect. C* **1984**, *C40*, 781.

(46) Beall, G. W.; Milligan, W. O.; Wolcott, H. A. *J. Inorg. Nuclear Chem.* **1977**, *39*, 65.

(47) Parker, D.; Dickins, R. S.; Puschmann, H.; Crossland, C.; Howard, J. A. K. *Chem. Rev. (Washington, DC, U. S.)* **2002**, *102*, 1977.

(41) Kutlu, I.; Kalz, H. J.; Wartchow, R.; Ehrhardt, H.; Seidel, H.; Meyer, G. Z. *Anorg. Allg. Chem.* **1997**, *623*, 1753.

(42) Kutlu, I.; Meyer, G. Z. *Anorg. Allg. Chem.* **1999**, *625*, 402.

(43) Doert, T.; Rademacher, O.; Getzschmann, J. Z. *Kristallogr. New Cryst. Struct.* **1999**, *214*, 11.

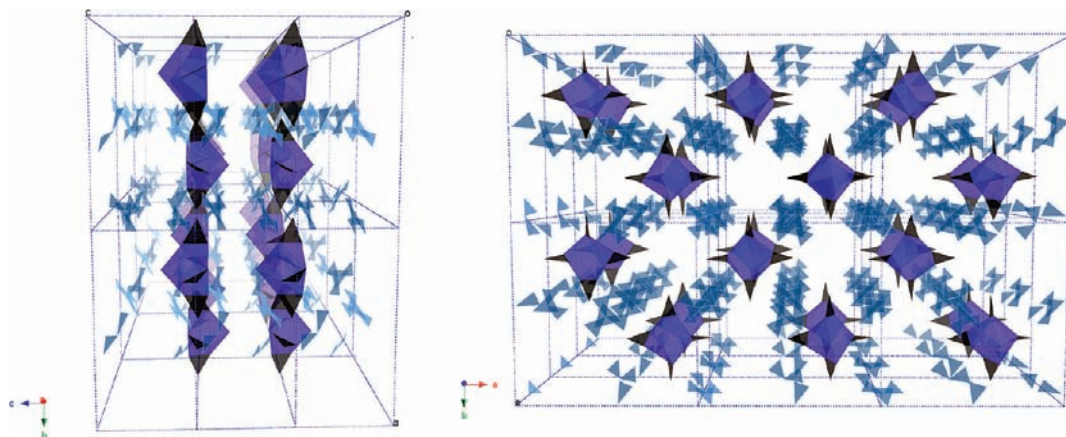


Figure 6. Packing illustration for the molecular structure of $[\text{C}(\text{NH}_2)_3]_4[\text{Dy}(\text{CO}_3)_4(\text{H}_2\text{O})](\text{H}_3\text{O}) \cdot 13\text{H}_2\text{O}$ (**II**) along the a axis (left) and c axis (right). $[\text{DyO}_9]$ groups are denoted by purple polyhedra, black triangles indicate $[\text{CO}_3]$ groups, and light blue groups represent guanidinium groups $[\text{C}(\text{NH}_2)_3]$. (Water molecules are not included.)

in this review. Due to the overlap in the reported bond lengths for Dy compounds with coordinated hydroxide ligands or water molecules in the literature, an accurate determination of the nature of the Dy–O4 bond based solely on X-ray diffraction data is difficult. Therefore, we must turn to other characterization techniques, such as vibrational spectroscopy, to determine if O4 is a coordinated hydroxide or a water molecule.

We have studied the solid-state Raman spectrum of **II** in order to look for active vibrational modes that would indicate that O4 is a coordinated hydroxide ion. Metal hydroxides (MOH) typically exhibit active Raman bands for the M–OH stretching modes at about 3600 cm^{-1} and M–OH bending and deformation modes below 1200 cm^{-1} .^{48–51} A vibrational study using Raman spectroscopy was reported for the trihydroxide complexes of the form $\text{Ln}(\text{OH})_3$ with symmetry analysis and vibrational mode assignments for each of the observed peaks.⁵² The authors reported that the primary peaks in the solid phase for $\text{Dy}(\text{OH})_3$ occur at 3597 , 696 , 504 , and 395 cm^{-1} and that these four peaks are all sharp and relatively narrow bands (less than 200 cm^{-1} width for the broadest peak at 504 cm^{-1}). Figure 7 below shows the Raman spectrum for solid samples of both guanidinium carbonate and **II**, along with the location of the peaks from $\text{Dy}(\text{OH})_3$. The spectrum for **II** does not exhibit any significant peaks in the regions near those reported for $\text{Dy}(\text{OH})_3$, indicating that O4 is in fact a coordinated water molecule and not a hydroxide ligand. The broad peaks at 3000 – 3700 cm^{-1} belong to vibrational stretches in the lattice waters in **II**, and the sharp peaks from 1040 to 1060 cm^{-1} result from the coordinated carbonate ligands. These modes are shifted to slightly higher wavenumbers when compared to the peaks in pure guanidinium carbonate due to the inner-sphere coordination of Dy atoms with carbonate ligands.

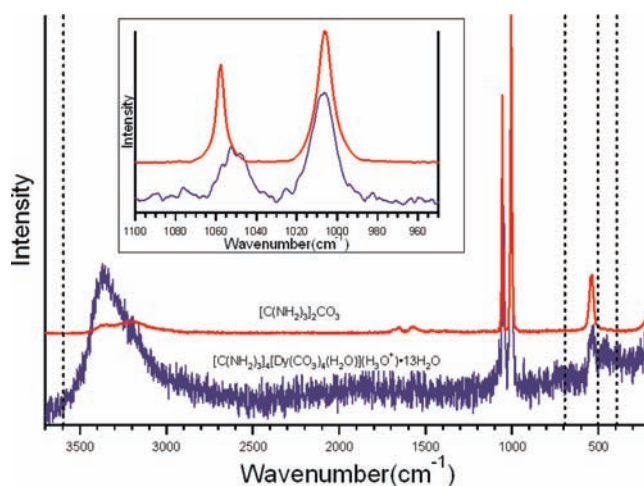


Figure 7. Raman spectra of $[\text{C}(\text{NH}_2)_3]_4[\text{Dy}(\text{CO}_3)_4(\text{H}_2\text{O})](\text{H}_3\text{O}) \cdot 13\text{H}_2\text{O}$ (**II**) (in blue), showing no characteristic OH^- signatures when compared to $\text{Dy}(\text{OH})_3$ (dashed lines),⁵² indicating the bound O4 atom belongs to a coordinated water molecule. The inset shows that the carbonate vibrational peaks (1040 – 1060 cm^{-1}) have shifted slightly when compared to that of guanidinium carbonate (in red).

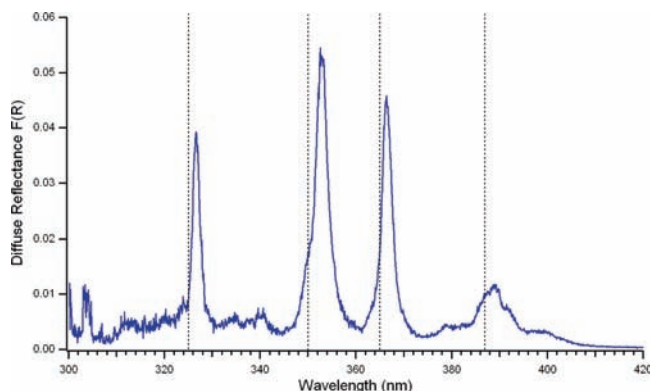


Figure 8. Spectroscopic features of the UV–vis–NIR diffuse reflectance spectrum (solid line) of $[\text{C}(\text{NH}_2)_3]_4[\text{Dy}(\text{CO}_3)_4(\text{H}_2\text{O})](\text{H}_3\text{O}) \cdot 13\text{H}_2\text{O}$ (**II**), indicating small shifts in the primary reflectance peaks relative to the four most intense transitions in the absorbance spectrum for the Dy^{3+} aquo ion (dashed line).⁴⁰

(48) Phillips, B. A.; Busing, W. R. *J. Phys. Chem.* **1957**, *61*, 502.

(49) Busing, W. R. *J. Chem. Phys.* **1955**, *23*, 933.

(50) Nakamoto, K. *Infrared and Raman Spectra of Inorganic and Coordination Compounds, Part A: Theory and Applications in Inorganic Chemistry*; 6th ed.; Wiley-Interscience: New York, 2009.

(51) Nakamoto, K. *Infrared and Raman Spectra of Inorganic and Coordination Compounds, Part B: Applications in Coordination, Organometallic, and Bioinorganic Chemistry*; 6th ed.; Wiley-Interscience: New York, 2009.

(52) Swanson, B. I.; Machell, C.; Beall, G. W.; Milligan, W. O. *J. Inorg. Nuclear Chem.* **1978**, *40*, 694.

Additional characterization of **II** was performed using conventional UV–vis–NIR diffuse reflectance spectroscopy. The electronic absorbance spectrum for Dy^{3+} is

characterized by fewer Laporte-forbidden $f-f$ transitions in the visible region from 400 to 800 nm compared to the spectrum of Er^{3+} .⁴⁰ Figure 8 shows a comparison of the solid state diffuse reflectance spectrum for **II** along with the significant $f-f$ transitions in the Dy^{3+} aquo ion absorbance spectrum. Three intense reflections for $[\text{C}(\text{NH}_2)_3]_4[\text{Dy}(\text{CO}_3)_4(\text{H}_2\text{O})](\text{H}_3\text{O}) \cdot 13\text{H}_2\text{O}$ can be seen at 326.6, 352.9, and 366.4 nm and a broad band at about 388 nm. This sequence is also present in the absorption spectrum for the Dy^{3+} aquo ion; however, the three primary absorbance peaks are shifted by +1.6, +2.9, and +1.4 nm due to the complexation of Dy^{3+} with carbonate.

Conclusions

Single crystals have been synthesized and characterized by X-ray diffraction studies for the tetra-carbonates of Er(III) and Dy(III), $[\text{C}(\text{NH}_2)_3]_5[\text{Er}(\text{CO}_3)_4] \cdot 11\text{H}_2\text{O}$ (**I**) and $[\text{C}(\text{NH}_2)_3]_4[\text{Dy}(\text{CO}_3)_4(\text{H}_2\text{O})](\text{H}_3\text{O}) \cdot 13\text{H}_2\text{O}$ (**II**). These compounds represent the first molecular structures of Er and Dy carbonates, as well as the first crystal structures containing binary carbonate moieties for these lanthanides. The structures reported herein provide insight into the coordination chemistry and solubility limiting species in concentrated carbonate

solutions and the different coordination chemistries between light and heavy lanthanides. The Dy(III) in **II** exhibits the nine-coordinate geometry observed in the analogous Nd(III) compound, $[\text{C}(\text{NH}_2)_3]_5[\text{Nd}(\text{CO}_3)_4(\text{H}_2\text{O})] \cdot 2\text{H}_2\text{O}$,¹⁰ the heavier lanthanide Er(III) in **I** is only eight-coordinate, which is similar to the Ho(III) compound, $[\text{Co}(\text{NH}_3)_6][\text{Na}_2(\text{H}_2\text{O})_{10}][\text{Ho}(\text{CO}_3)_4] \cdot 4\text{H}_2\text{O}$.¹¹ The nature of the coordinated water molecule in **II** was explored with Raman spectroscopy, which did not show any evidence for the presence of a coordinated hydroxide. These structures provide the basis to probe the effect of ionic radius on the nature of the limiting solution species in concentrated carbonate solutions, which is the subject of a manuscript currently in preparation.

Acknowledgment. We would like to thank Dr. F. Caporuscio for many helpful discussions. This research was funded by the Los Alamos Laboratory Directed Research and Development Program, the U.S. Department of Energy Fuel Cycle R&D Program, and the G. T. Seaborg Institute for Transactinium Science at Los Alamos National Laboratory.

Supporting Information Available: Complete crystallographic details in CIF format are provided. This material is available free of charge via the Internet at <http://pubs.acs.org>.